

LHC Probe of Quark Substructure at the Early Stages of Running

Z. Usubov*

Dzhelepov Laboratory of Nuclear Problems,
Joint Institute for Nuclear Research,
141980, 6 Joliot-Curie, Dubna, Moscow Region, Russia

December 11, 2018

Abstract

We explore the opportunity to look for quark compositeness in the early stages of the LHC running by analyzing high- E_T dijet production. The quark substructure that will manifest itself by affecting various kinematic distributions at the center-of-mass energy $E_{cm}=10$ TeV and in the integrated luminosity range from 0.5 to 10 fb $^{-1}$ is investigated. The estimation of the characteristic energy scale Λ , based on the novel, potentially powerful observable, is found to be sensitive to the sign of the interference between Standard Model and four-fermion contact interactions. We find the lower limits on Λ at the LHC to be about 10.5(15.0) TeV for constructive interference and 8.5(11.5) TeV for destructive one at the integrated luminosity 0.5(10) fb $^{-1}$ and $E_{CM} = 10$ TeV.

1 Introduction

Tremendous effort in the LHC experiments will be made to reveal the origin of electroweak symmetry breaking. The agent of the symmetry breaking, as is formulated in the Standard Model (SM), is a scalar field giving rise to one physical neutral scalar Higgs boson. On the other hand, the electroweak symmetry breaking can also arise from QCD-like interacting sector of composite particles (with a fermion antifermion condensate $\langle \bar{\psi}\psi \rangle \neq 0$ breaking the symmetry). Indeed, the existence of too many free parameters in the SM and three families of quarks and leptons could be an indication of the substructure of these objects.

At the energies much below the characteristic energy scale Λ with the neglect of the underlying strong dynamics a new coupling among quarks can be approximated by a four-fermion

*On leave of absence from Institute of Physics, Baku, Azerbaijan

contact interactions. A search for evidence for the quark substructure is usually based on the concept of their higher dimensional operator contribution leading to the contact interaction term in the effective Lagrangian of the form[1]

$$L_{qq} = \lambda \frac{g^2}{2\Lambda^2} [\bar{q}\gamma^\mu q][\bar{q}\gamma_\mu q] \quad (1)$$

where $\lambda = -1(+1)$ defines constructive (destructive) interference between the contact and SM interactions and g^2 is the quark compositeness coupling constant. The compositeness energy scale Λ can be chosen such that $\frac{g^2}{4\pi} = 1$, and the model is completely determined by specifying the parameters λ and Λ .

A typical signal of quark compositeness would be an excess of the high- E_T jets over the level predicted by QCD and/or a more isotropic dijet angular distribution than what is expected from the SM.

The current experimental lower limits on the quark compositeness scale from lepton-lepton, lepton-nucleon and nucleon-nucleon interactions vary from 2.5 to 6.3 TeV[2, 3, 4], depending on the chirality channels under consideration.

The expected sensitivity of the ATLAS experiment to the discovery of the contact interactions can be found in[5]. Prospects for a luminosity and energy upgraded LHC are also presented[6]. The possibility of the composite top quark manifestation at the LHC is now widely discussed[7].

The rest of this note is organized as follows. In Section 2 we describe all the observables that we use to study the quark compositeness. Section 3 gives a brief description of the data simulation technique. Section 4 gives a summary of our analysis itself. We examine the effect of the quark substructure on the measurables and the sensitivity of the data to the quark compositeness scale. The sensitivity of the results to the parton distribution functions (pdfs) is also demonstrated in Section 4. Section 5 presents our conclusions.

2 Quark substructure observables at the LHC

The LHC allows one to reach very large values of jet transverse energy ($E_T > 1.5$ TeV) and dijet invariant mass ($m_{j1j2} > 3.0$ TeV) even in the early stages of operation. Such a kinematic region of dijet production has never been studied before.

To study dijet properties in pp collisions at the center-of-mass energy $E_{CM} = 10$ TeV, we chose four variables:

- P_T distribution of two most energetic jets;
- χ , defined as $\chi \equiv \exp |\eta_1 - \eta_2|$, where $\eta_{1,2}$ are the pseudorapidities of two leading jets. For the case of $2 \rightarrow 2$ parton scattering χ is related to the center-of-mass scattering angle θ^* as

$$\chi = \frac{1 + |\cos\theta^*|}{1 - |\cos\theta^*|}; \quad (2)$$

- α_R , which was proposed by L. Randall and D. Tucker-Smith[8] as the ratio of the second hardest jet transverse momentum and the invariant mass m_{j1j2} of two hardest jets

$$\alpha_R \equiv \frac{P_{T_2}}{m_{j1j2}}; \quad (3)$$

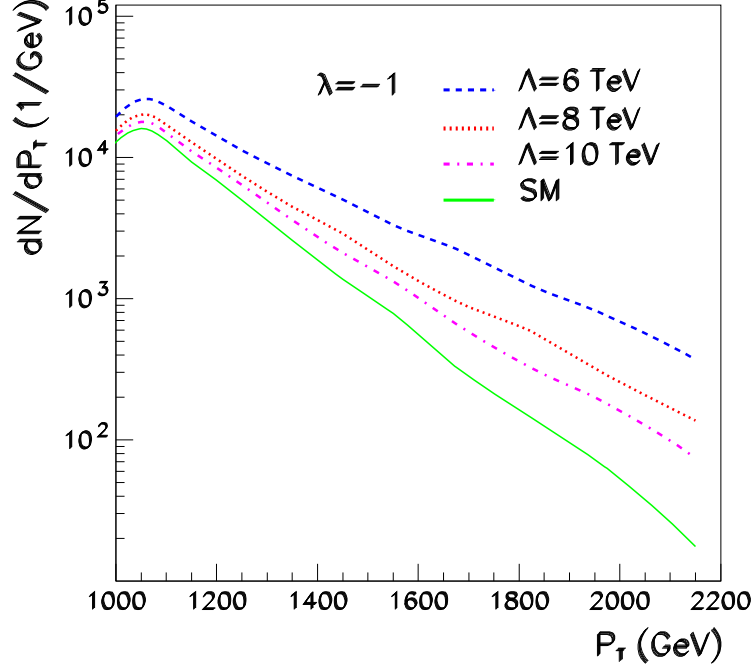


Figure 1: P_T distribution of two leading jets for the Standard Model and the composite quark predictions at different energy scales Λ and $E_{CM} = 10$ TeV. The data correspond to the constructive interference between the Standard Model and the contact interactions.

- the dimensionless variable α_Z , which we define as $\frac{E_{CM}}{2}$ times the ratio of the sum and the product of the transverse momenta of two hardest jets.

$$\alpha_Z \equiv \frac{E_{CM}}{2} \frac{P_{T_1} + P_{T_2}}{P_{T_1} \cdot P_{T_2}}. \quad (4)$$

The variable χ is defined through angular quantities, and hence is less susceptible to the precise knowledge of jet energy scale but it is sensitive to the gluon radiation and higher-order corrections. The use of the χ as a dijet angular distribution variable makes the comparison with theory more straightforward[9].

In fact, the variable α_R was introduced for dijet SUSY searches and QCD background suppression[8]. We find that this kinematic variable can be used in the quark compositeness study as well. The QCD induced $2 \rightarrow 2$ events have α_R distribution which sharply decreases around ~ 0.5 . The α_R distribution of the events with the contact interaction contribution has different behaviour near ~ 0.5 .

For our previous estimations of the compositeness scale Λ at the LHC[5] we considered the variable R_χ [10]

$$R_\chi = \frac{N(\chi < \chi_0)}{N(\chi > \chi_0)}, \quad (5)$$

which is the ratio of the number of dijet events with $\chi < \chi_0$ to the number of dijet events with $\chi > \chi_0$. This single parameter is helpful for describing the whole χ distribution. The

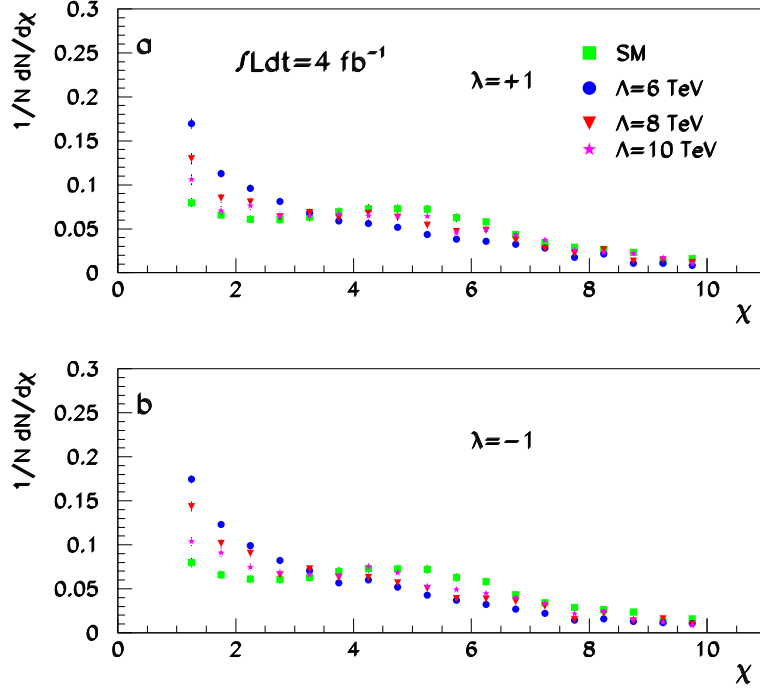


Figure 2: Dijet angular distributions for the Standard Model prediction compared to the quark contact interaction predictions at different energy scales Λ and $E_{CM} = 10$ TeV. The integrated luminosity is assumed to be 4 fb^{-1} : a) destructive interference term; b) constructive interference term.

appropriate choice of χ_0 maximizes the sensitivity of the variable R_χ to the features of the χ distribution.

The estimation of Λ in this study is based on the analysis of α_Z . As in the case of the variable χ , to describe the whole distribution with a single parameter, we constructed the variable

$$R_{\alpha_Z} = \frac{N(\alpha_Z < \alpha_Z^0)}{N(\alpha_Z > \alpha_Z^0)}, \quad (6)$$

where $N(\alpha_Z > \alpha_Z^0)$ ($N(\alpha_Z < \alpha_Z^0)$) is the number of dijet events with $\alpha_Z > \alpha_Z^0$ ($\alpha_Z < \alpha_Z^0$).

In order to know to what extent the observations either conform or disprove the quark compositeness scenario we consider the significance

$$S = \frac{R_{\alpha_Z}(\Lambda) - R_{\alpha_Z}(SM)}{\sigma}, \quad (7)$$

where $\sigma = \sqrt{\sigma_\Lambda^2 + \sigma_{SM}^2}$.

It must be stressed that the distribution of $|\phi_1 - \phi_2|$, where $\phi_{1,2}$ are the azimuthal angles of the leading jets, for events with composite quarks show deviations from the SM prediction. This deviation depends on the compositeness scale Λ but is significantly smaller than that of the χ , α_R or α_Z distributions.

3 Data simulation for generic LHC detector

The simulation of the pp collision with a quark substructure scenario was performed with the event generator PYTHIA6.4[11]. We employ the leading-order CTEQ6L1[12] pdfs everywhere unless otherwise stated ¹. The initial-state and final-state QCD and QED radiation and multiple interactions were enabled. We choose the case where all quarks are composite. The model with the left-left isoscalar contact interaction term is supposed[1]. The events were generated with the hard subprocess transverse momentum $p_T > 1$ TeV.

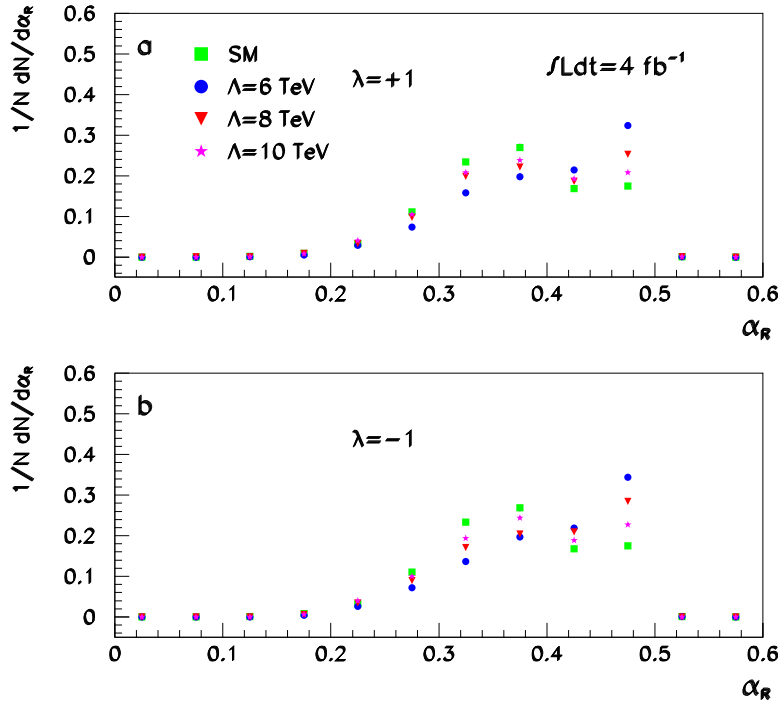


Figure 3: Normalized α_R distributions (see the text) for the Standard Model predictions compared to the quark contact interaction predictions at different energy scales Λ and $E_{CM} = 10$ TeV. The integrated luminosity is assumed to be 4 fb^{-1} : a) destructive interference term; b) constructive interference term.

The detector performance was simulated by using the publicly available PGS-4[14] package written by J. Conway and modified by S. Mrenna for the generic LHC detector. The calorimeter granularity is set to $(\Delta\phi \times \Delta\eta) = (0.10 \times 0.10)$. Energy smearing in the hadronic calorimeter of the generic LHC detector is governed by²

$$\frac{\Delta E}{E} = \frac{0.6}{\sqrt{E}} + 0.03 \quad (E \text{ in GeV}). \quad (8)$$

¹We used PYTHIA6.4 default choices for Q^2 definition as well as factorization and renormalization scales

²We add the constant term in the PGS-4 simulation of energy smearing in the hadronic calorimeter

Jets were reconstructed down to $|\eta| \leq 3$ using the k_T algorithm implemented in PGS-4. We chose $D = 0.7$ for the jet resolution parameter and required that $E_T(\text{jet}) > 100 \text{ GeV}$. We use the simplified output from PGS-4, namely, a list of two most energetic jets. The average P_T and invariant mass of the leading jets are $\langle P_T^{j1} \rangle = 1.12 \text{ TeV}$, $\langle P_T^{j2} \rangle = 1.01 \text{ TeV}$, $\langle m_{j1j2} \rangle = 2.46 \text{ TeV}$, respectively.

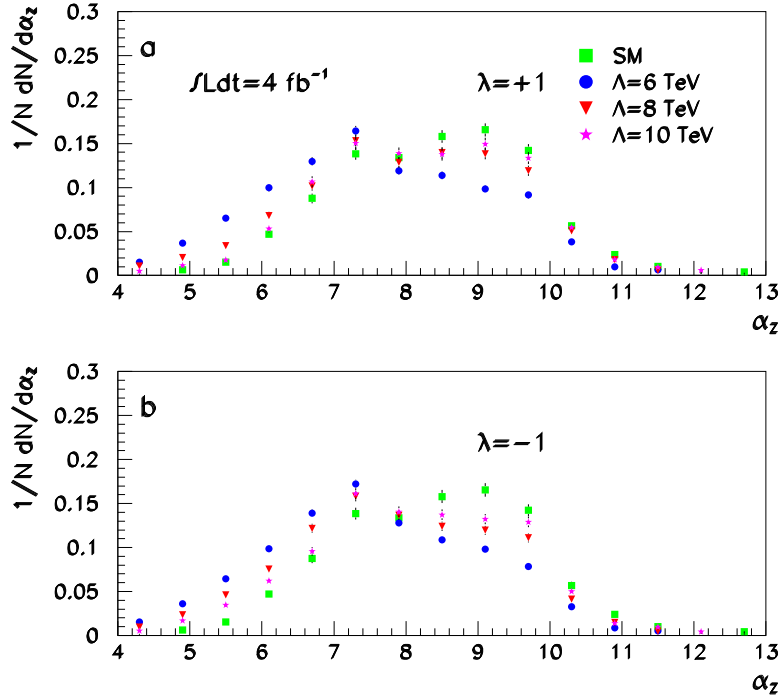


Figure 4: Normalized α_Z distributions (see the text) for the Standard Model predictions compared to the quark contact interaction predictions at different energy scales Λ and $E_{CM} = 10 \text{ TeV}$. The integrated luminosity is assumed to be 4 fb^{-1} : a) destructive interference term; b) constructive interference term.

4 What we are going to look for

Measurements of particle production at a very high transverse momentum at the LHC will provide a broad domain for new physics discovery. It has already been noted that the quark compositeness can be tested by looking for deviations of the jet transverse momentum distribution from the QCD prediction. In Fig. 1 we plot the P_T distributions for two leading jets predicted by the SM as well as by the quark substructure effect with different compositeness scale Λ . The data were simulated with constructive ($\lambda = -1$) interference term. Evidently, effect of quark substructure dominates over SM behaviour for high P_T jets.

The effect of quark compositeness is most pronounced in the high dijet mass region[5]. For further analysis the events are chosen to have $m_{j1j2} > 2.7 \text{ TeV}$. After applying this cut to leading

jets we have $\langle P_T^{j1} \rangle = 1.27 \text{ TeV}$, $\langle P_T^{j2} \rangle = 1.18 \text{ TeV}$, $\langle m_{j1j2} \rangle = 3.23 \text{ TeV}$, respectively.

The comparison of the dijet angular distribution predicted by the SM and induced by the quark substructure with different values of Λ is shown in Fig. 2. Plots *a* and *b* correspond to the normalized χ distributions, $(1/N)(dN/d\chi)$, for destructive and constructive interference, respectively. More isotropic angular distribution in the composite quark interactions lead to the χ distribution which peaked at low χ .

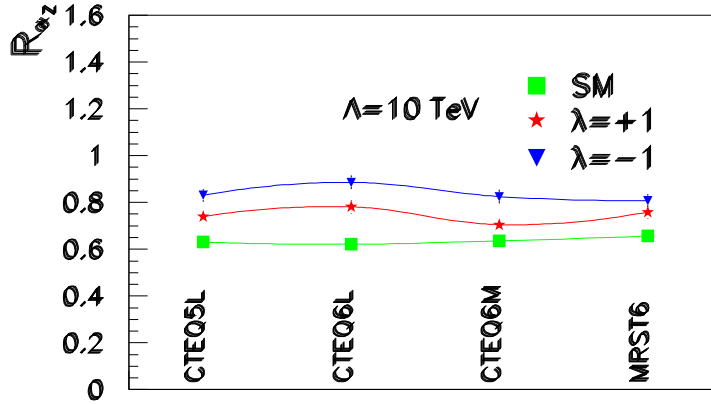


Figure 5: The dependence of R_{α_Z} (see the text) on the parton distribution functions. The compositeness energy scale is set to be $\Lambda = 10 \text{ TeV}$. The integrated luminosity is assumed to be 4 fb^{-1} and $E_{CM} = 10 \text{ TeV}$.

The normalized α_R distributions for destructive and constructive interference are demonstrated in Fig. 3 *a* and *b*, respectively. As becomes apparent from Fig. 3, quark compositeness leads to an enhancement (abatement) in the distribution at $\alpha_R > 0.4$ ($\alpha_R < 0.4$) in comparison to the SM prediction. In Fig. 4 we show the normalized α_Z distributions for destructive (a) and constructive (b) interference. The change in the behaviour of the α_Z distributions in the vicinity of $\alpha_Z = 8$ is quite impressive. The data sensitivity in Figs. 2, 3 and 4 corresponds to the integrated luminosity of 4 fb^{-1} .

The distributions of the variables χ , α_R and α_Z show a robust signal and can be used independently to observe effects from the quark substructure. One can see that the effect from quark compositeness is higher for constructive interference than for destructive one.

One of the main uncertainties in the interpretation of new physics at the LHC detectors will come from pdfs. Unfortunately, the pdfs are not so well determined in the kinematic region with high transverse momentum jets. Figure 5 shows the effect of the pdfs choice on the differences between the SM and composite quarks predictions for R_{α_Z} . The result obtained with the leading-order CTEQ6L1[12] parametrization is compared with the results which correspond to the leading-order CTEQ5L1[12] and next-to-leading order CTEQ6M1[12] and MRST 2006[13] pdfs. We can conclude that the LHC potential for the quark substructure study can be slightly affected by pdfs uncertainties.

In Fig. 6 we show the LHC lower limits on Λ up to which the effects of quark compositeness can be observed at $E_{CM} = 10 \text{ TeV}$ as a function of the accumulated luminosity. The data

correspond to the significance of eq.(7) close to $S=3$, for which we can claim that we have strong evidence for the observed signal. The parameter α_Z^0 used here is $\alpha_Z^0 = 8.0$. The data were obtained with the inclusion of statistical uncertainties alone. We performed analogous analysis of lower limits on Λ with the use of the variables χ and α_R . The estimates of Λ agree with those obtained with the use of α_Z within the ± 0.5 TeV gate. We find that with the LHC running at the design center-of-mass energy $E_{CM} = 14$ TeV, one will have a gain of ~ 0.5 TeV to the values of Λ obtained for $E_{CM} = 10$ TeV at the integrated luminosity in the range from 0.5 to 10 fb^{-1} . For this analysis we used $m_{j_1 j_2} > 3.0$ TeV.

5 Conclusions

We examined the capability of the LHC experiments to observe quark substructure in the early stages of the running considering that the LHC would have an accumulated luminosity in the range from 0.5 to 10.0 fb^{-1} at $E_{CM} = 10$ TeV.

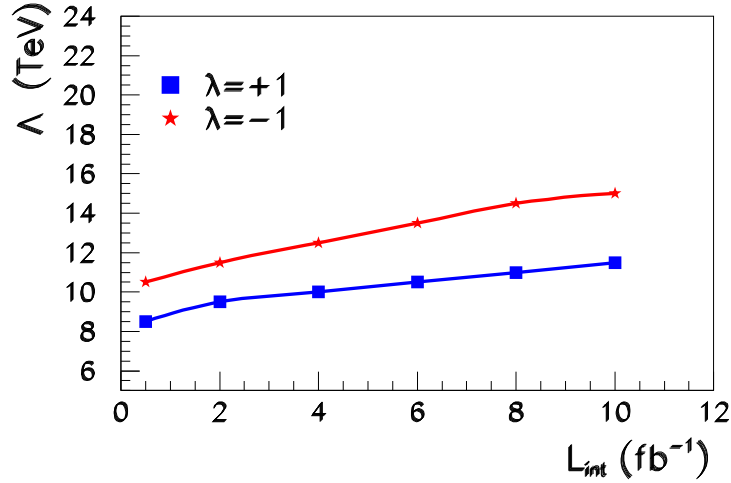


Figure 6: LHC reach on the characteristic energy scale Λ as a function of the integrated luminosity for constructive ($\lambda = -1$) and destructive ($\lambda = +1$) interference term and $E_{CM} = 10$ TeV.

We show that quark compositeness at the LHC can be manifested by different dijet kinematic variables. The distribution of two novel variables α_R [8] and α_Z might provide direct hint to the quark substructure observation as well as dijet transverse momentum and angular distributions. Analysis of the variable α_Z defined in the paper can be effective for estimation of the compositeness energy scale Λ . In the early stages of the LHC running it is possible to probe the compositeness scale Λ up to 10.5(15.0) TeV for the constructive interference term and 8.5(11.5) TeV for the destructive one for the integrated luminosity of 0.5(10) fb^{-1} and $E_{CM} = 10$ TeV.

The last but not the least, such a features of the transverse momenta and angular distribution for high energy jets can have different new physics sources (SUSY, extra dimensions, Technicolor etc.). In this case the use of combinations of observables will be most effective for the discrimination and interpretation of the data and the understanding of the underlying theory.

References

- [1] E. Eichten, K. Lane and M.E. Peskin, Phys.Rev.Lett. 50, 811 (1983);
E. Eichten, I. Hinchliffe, K. Lane, C. Quigg, Rev.Mod.Phys. 56, 579 (1984);
ibid., 58, 1065 (1986).
- [2] G. Abbiendi et al. (OPAL Collab.), Eur.Phys.J. C33, 173 (2004), hep-ex/0309053;
M. Acciarri et al. (L3 Collab.), Phys.Lett. B489, 81 (2000), hep-ex/0005028.
- [3] C. Adloff et al., (H1 Collab.), Phys.Lett. B479, 358 (2000), hep-ex/0003002.
- [4] J.A. Green, FERMILAB-CONF-00-088-E, hep-ex/0004035.
- [5] ATLAS Collaboration, Detector and Physics Performance Technical
Design Report, CERN/LHCC/99-15, V.II, p.932.
- [6] F. Gianotti et al., Eur.Phys.J. C39, 293 (2005), hep-ph/0204087;
G. Azuelos et al., J.Phys. G28, 2453 (2002), hep-ex/0203019.
- [7] K. Agashe, R. Contino, R. Sundrum, Phys.Rev.Lett. 95, 171804 (2005), hep-ph/0502222;
B. Lillie, J. Shu, T.M.P. Tait, JHEP 0804, 087 (2008), arXiv:0712.3057[hep-ph];
A. Pomarol, J. Serra, Phys.Rev. D78, 074026 (2008), arXiv:0806.3247[hep-ph];
K. Kumar, T.M.P. Tait, R. Vega-Morales, arXiv:0901.3808[hep-ph].
- [8] L. Randall and D. Tucker-Smith, Phys.Rev.Lett. 101, 221803 (2008),
arXiv:0806.1049[hep-ph].
- [9] V. Barger and R.J.N. Phillips, Collider Physics, Addison-Wesley,
Redwood City, CA, 1987.
- [10] F. Abe et al., (CDF Collab.), Phys.Rev.Lett. 77, 5336 (1996), Erratum-ibid. 78, 4307 (1997),
hep-ex/9609011.
- [11] T. Sjöstrand, S. Mrenna, P. Skands, JHEP 0605, 026 (2006).
- [12] J. Pumplin et al., JHEP 0207, 012 (2002), hep-ph/0201195.
- [13] A.D. Martin, W.J. Stirling, R.S. Thorne, and G. Watt, Phys. Lett. B652, 292 (2007),
arXiv:0706.0459.
- [14] PGS-4, Simulation package for generic collider detectors
<http://www.physics.ucdavis.edu/~conway/research/software/pgs/pgs.html>